参赛学生姓名：王 雨 昕

中学：南 京 外 国 语 学 校

省份：江 苏

国家/地区：中 国

指导老师姓名：李 曙

指导老师单位：南 京 外 国 语 学 校

论文题目：Multi-finger Gesture Recognition with Magnetic Sensing on Mobile Devices

Multi-finger Gesture Recognition with Magnetic Sensing on Mobile Devices

YUXIN WANG, Nanjing Foreign Language School, China

Abstract: In this project, we explore the possibility of wearing small magnets on fingernails to allow users to interact with mobile devices dexterously using multiple fingers. Specifically, we use ultra-thin Halbach magnets that have distinctive magnetic field distributions at different distances and directions. By wearing the magnet in different orientations on different fingers, we can recognize the same set of five gestures performed by each of the two fingers with high accuracy. Moreover, we discover that the wearable magnets enable the magnetometer to sense the user's heartbeat through the small vibration of fingertips.

Additional Key Words and Phrases: Human-Computer Interaction, Gesture Recognition, Magnetic Sensing

1 INTRODUCTION

Nowadays, our daily life is increasingly occupied by personal mobile devices, including mobile phones, smart watches, and AR/VR devices. How to efficiently interact with these devices has become an important research issue in the Human Computer Interaction (HCI) area. The touch screen, which is the currently dominating solution to interaction with mobile devices, has its own limitations. First, due to the large sizes and high costs of touch screens, small devices (such as smart watches or earphones) could not support convenient touchscreen-based input. Second, the touchscreen combines the input with the display function, so users have to look at the device when performing input and touching the screen may occlude the content of display.

As envisioned by Vernor Vinge in his famous science fiction "Rainbows end", younger generations might invent and quickly master complex gesture interactions when the device can precisely track the movement of fingers in the air. To enrich the users' interaction experience, researchers have explored different solutions to in-the-air gesture recognition, using wireless signals [1] or cameras [2]. However, the high multipath interference leads to possible tracking errors for solutions using wireless signals, such as Wi-Fi and mmWave. Camera-based gesture recognition systems require high energy and considerable computational power cost, so they are not well suited for mobile devices.

One of the possible solutions for gesture recognition is magnetic sensing. As low-cost magnetometers are universally used in devices, most mobile equipment, including smart watches, AR/VR, and earphones, can precisely measure the surrounding magnetic field. Researchers have embedded permanent magnets in objects, such as styluses [3], to perform tracking. However, it is harder for users to manipulate the objects for HCI than directly using their fingers. There are proposals of placing magnets on rings. But, rings are worn near the root of the finger, so they cannot reflect the dexterous movement of finger tips. Existing solutions to wearing conventional permanent magnets on finger tips is cumbersome [4, 5], where the size of the magnets is around 3 mm thick and 10 mm in diameter.

In this project, we explore the possibility of using wearable Halbach array magnets for gesture recognition. Our solution has the following distinctive features. First, the Halbach magnet can be made extremely small. The magnet used in our design has a thickness of only 0.7 mm with a size of just 3.44 mm×6.68 mm. With such a small form-factor, the magnet could be easily placed under the popular wearable fingernails and could last for weeks since placed. Second, the Halbach magnet is composed of multiple small magnets, so the magnetic field distribution alters based on the structure of the array. The magnetic field shows different features in different orientations. Therefore, we can place magnets with different orientations on different fingers to distinguish fingers using the specific field features. Furthermore, the composition of the Halbach magnet increases the magnetic field strength close to the magnet and reduces the magnetic field strength far from the magnet. Thus, even if two

Author's address: Yuxin Wang, felicia_wang@foxmail.com, Nanjing Foreign Language School, Nanjing, China.

fingers are only a few centimeters to each other, the magnetic field of the closer finger will dominate and the interference between fingers will be reduced. With the help of the Halbach magnets, we are able to recognize a set of ten gestures performed by different fingers within a distance of 5 cm to the device. More interestingly, we discover that we can also sense the heartbeat of the user when the user places the finger, its nail attached to the Halbach magnet, on the surface of the phone. It shows the sensitivity of our magnetic-based sensing approach.

To enable reliable magnetic sensing, our project addresses the following technical challenges. First, it is well known that the magnetometer is hard to calibrate [6]. The readings of magnetometer on mobile devices are easily interfered by the magnetic field of the earth and nearby iron objects, so the readings may dramatically change because of the surrounding environment. To solve this problem, we use the accelerometer as reference to determine the time instances that the device is not moving, then use the static magnetic field as a reference. Furthermore, we use features that depend on the change of the field rather than the absolute readings in gesture recognition for better robustness. Second, the magnetic fields of magnets on different fingers may interfere with each other when fingers are performing complex gestures. To avoid such interference, we design specific gesture sets so that each gesture has distinguish field change patterns to avoid recognition errors. With our simple gesture design, we can use low-complexity algorithms such as nearest neighbor to achieve high recognition accuracy. Third, the readings of magnetometer is noisy, and useful information such as the heartbeat signal could be buried in the noise. To address this problem, we first use the moving average approach to remove both fast fluctuations and the trend in the signal so that small variations can be recovered. We also design a set of robust features that focus on the changes in the magnetic direction to remove the impact of drastic changes in the amplitude of the field when the distance between the magnet and the magnetometer changes.

In summary, the main contribution of this project is as follows:

- To our best knowledge, this project is the first one that uses small Hallbach magnets to perform magnetic field based gesture recognition.
- We revealed the key features of Halbach magnets and designed multi-finger gestures accordingly. We also discovered that it is possible to recognize the heartbeat of the user with magnets worn on finger tips.

2 RELATED WORK

The most related researches to this work can be categorized into the following three areas: magnet-based object tracking, wearable magnetic devices, and device-free gesture tracking.

Magnet-based Object Tracking: Magnetic field based sensing have been widely used for tracking objects. Bianchi *et al.* [7] and Zheng *et al.* [8] both design toys with permanent magnets embedded in them to facilitate human-computer interaction with objects. ProxiFit uses magnetic sensing to track iron objects, *e.g.,* dumbbells, during exercises [9]. Magnets have also been used on styluses to perform 2D drawing on mobile devices [3, 10, 11] or Virtual Reality devices [12]. MagSound combines the magnetic field and the sound field of an earphone to perform 2D tracking of the earphone [13]. While these solutions provide fine-grained 2D tracking of magnet embedded objects, the interactions are conducted via a separate physical object. Such object-oriented interactions are not as flexible as finger-tip based interactions.

Wearable Magnetic Devices: Recent researches in HCI also explore various methods of attaching magnets to human bodies. Magnets on rings have been used for user authentication [14–16]. However, since rings are usually worn at the root of fingers, the inflexible movement lead to limited gestures enabled by magnetic rings [17]. Harrison *et.al.* [4], Lyons [5], and Chan [18] proposed to attach a permanent magnet to the finger tip. However, the magnet used in these works has a diameter of one centimeter, which means it is impractical to attach the magnet to finger tips for a long time. Other similar approach attach objects on finger tips have similar size problems [19–22]. Moreover, the proposed solution only allows tracking of a single finger. Finexus uses coils attached to multiple fingers to distinguish different fingers [23]. However, the coils needs power and the devices are even larger than permanent magnets.

Device-free Gesture Tracking: There are other solutions to perform in-the-air gesture tracking using mobile devices. FingerIO use ultrasound to track finger movements around smartwatches [24]. Smartphones can also track user gestures using millimeter waves [25] or Wi-Fi signals [26]. However, these sensing systems based on sounds or wireless signals are susceptible to multi-path interference, so they cannot reliably work in noisy environments. There are solutions that use cameras on smartwatches [27] or light reflections [28] to recognize gestures on mobile devices. Due to the high energy consumption for image capture and processing, these solutions could quickly drain the battery of mobile devices. There are wearable fingernails that has embedded small RFID chips [29]. But, RFID need specific readers that are not commonly avaiable on mobile devices.

3 SYSTEM MODEL

3.1 Motivation

Magnetic sensing has been widely used in different types of Human-Computer Interaction (HCI) scenarios [8, 9, 14]. As magnetic sensors are integrated into Inertial Measurement Unit (IMU) chips, most mobile devices can output 3D magnetic field measurements. By taking advantage of this “free” sensing capability, prototype systems embed permanent magnets into different types of objects, such as stylus, toys, and ear phones, to perform magnetic-based tracking. However, these applications do not fully relish the opportunity of magnetic-based gesture recognition by attaching magnets to human hands.

Human fingers are extremely flexible and dexterous. They can accurately perform many complex tasks. However, magnetic-based finger gesture sensing faces two major challenges that haven’t been solved by existing works. First, existing wearable solutions attach the cumbersome neodymium magnets on human fingers [5]. As these magnets are large, *e.g.*, nearly 3mm thick,it is impossible to wear these magnets on fingers in daily life, see Fig. 1(e). On the other hand, reducing the size of magnet may greatly reduce the strength of the magnetic field, so the magnetic sensor cannot reliably capture the signal. Second, existing solutions cannot distinguish different fingers. While the magnetic field decays faster than the electronic field [30], it is not decaying fast enough to enable distinguishing fingers that are no more than a few centimeters to each other.

In this project, we aim at using wearable magnets to enable flexible finger gestures. Our design is motivated by the above challenges. We propose to attach ultra-thin permanent magnets to multiple fingers of the user. A single magnetometer embedded in the mobile device can sense the mixed magnetic field of multiple magnets at the same time. We envision such finger-based wearable solution that enables new opportunities of gesture interaction. To address the two challenges of wearable magnets, we propose using special magnets instead of the common uniform neodymium magnets.

3.2 Magnet Selection

We propose using ultra-thin Halbach magnets for our wearable solution. Such magnets are widely used in foldable mobile phones and laptops to hold mobile parts of these devices in place. To fit in the small mobile phones, these Halbach magnets are usually very small, but they can create high magnetic field to generate forces strong enough to meet the mechanical design requirements.

As Fig. 1(a) shows, the Halbach magnets used in this project, which are scavenged from foldable mobile phones, are ultra-thin and small in size. The magnet, 6.68 mm in length and 3.44 mm in width, is small enough to attach to a fingernail. More importantly, the magnet is extremely thin, having a thickness of only 0.70 mm, which means it can be comfortably patched under wearable fingernails. In comparison, the uniform neodymium magnet used in [5] has a diameter of 10 mm and a thickness of nearly 3 mm, see Fig. 1(d). Such large form-factor of uniform neodymium magnets make them too cumbersome to be used in wearable devices.

(a) Halbach front view

(b) Halbach back view

(c) Halbach magnetic structure

(d) Uniform neodymium magnet

(e) Comparing different types of magnets

Fig. 1. Comparing the structure of Halbach magnet and uniform neodymium magnet

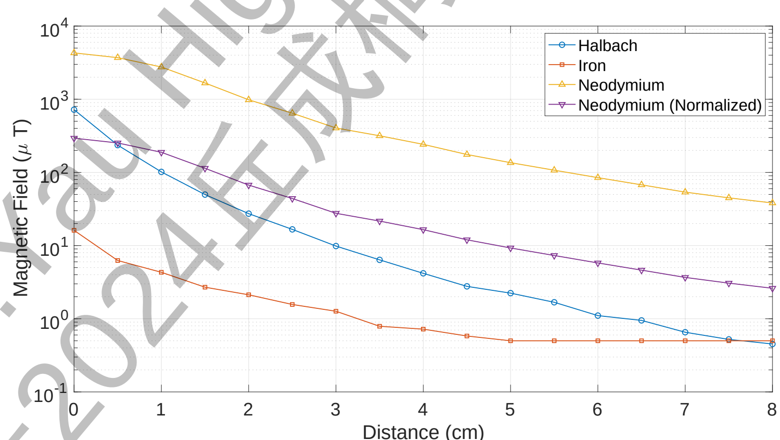

Fig. 2. Comparing the magnetic field strength of different magnets

Though the Halbach magnets used in this project are small in size, they create strong magnetic fields. Unlike uniform permanent magnets, the Halbach magnets are combinations of multiple small magnets to redistribute their magnetic field, as shown in Fig. 1(c). The different poles of small magnets, arranged in a specific way, alter the magnetic field of the Halbach magnet, usually increasing the strength of the field close to the magnet. To compare the magnetic field strength of different objects and to confirm that the field of the Halbach magnet is stronger, we measure the amplitude of magnetic field at different distances. Three types of objects are measured: the Halbach magnet in Fig. 1(a), the uniform neodymium magnet in Fig. 1(d), and a small piece of iron about the same size of the Halbach magnet. Fig. 2 shows the result of the measurement, where the field strength in μT is plotted in log scale. Note that the uniform neodymium magnet is much larger than the other two objects, having a volume of about 15 times that of the Halbach magnet. Therefore, we normalized the field of the uniform neodymium magnet by its volume, *i.e.*, divide the strength by 15 times.

Form Fig. 2, we have the following observations. First, the Halbach magnet has about the same field strength as the normalized neodymium magnet, while the fields of both magnets are much stronger than the iron's. The strength of the Halbach magnet reaches 10 μT at a distance of 3~4 cm to the sensor, which is comparable to the earth magnetic field background of around 22~65 μT. This hints that the field of the Halbach magnet can be reliably detected at a distance of 3~4 cm. Our measurement also shows that the background noise of the magnetic senor in mobile phone has an average amplitude of 0.5 μT in static environments. As the Halbach magnet generates a field strength of around 1 μT at a distance of 6 cm, the effective sensing range is about 6 cm, which is suitable for interaction with mobile phones, watches, or VR/AR devices. Second, the structure of the Halbach magnet changes the strength distribution of magnetic field. Compared to the normalized neodymium magnet, the field strength of the Halbach magnet is much stronger when the distance is small, while the field decays faster as the distance increases.

This modified field distribution is suitable for gesture sensing. Because the strong field near the magnet enables reliable detection of actions within a short distance to the device, especially when the finger is touching the device. The considerable change of the field strength allows the sensor to detect small movements, as the field strength changes a lot when the distance only changes a little. The fast decaying of the field is also preferable. This is because the field will be dominated by the nearest finger and the field of other fingers that are more than 6 cm to the device will be small enough to be ignored.

In summary, we find the Halbach magnet is a good choice for wearable magnetic sensing. It solve the two challenges mentioned in Sec. 3.1 by providing an ultra-thin magnet that generates a strong but fast-decaying field in a short distance to reliably detect the position and to avoid interference due to multiple magnets. Therefore, we choose to use the Halbach magnet in our wearable solution.

3.3 Magnetic Sensing Model

We use the magnetometer embedded in mobile devices to measure the field generated by the Halbach magnet. Specifically, we use iPhone as the sensing platform in this project.

The iPhone has an IMU senor that provides the acceleration, rotation, as well as magnetic measurement. For the mobile phone used in this project, an iPhone 13 mini, the IMU sensor is located at the up-left corner of the phone, as shown in Fig. 3. In our implementation, the sensor outputs 50 measurements each second. Each measurement contains the magnetic field measurements along three axes, X, Y, and Z, with direction shown in Fig. 3. In other words, each measurement is a vector with three float point values (H_x,H_y, and H_z) of magnet field measured in terms of μT. The three-axes measurement provides additional directional information on top of the strength of the magnetic field. The direction of field is very useful for identifying multiple magnets, as we will show in later sections.

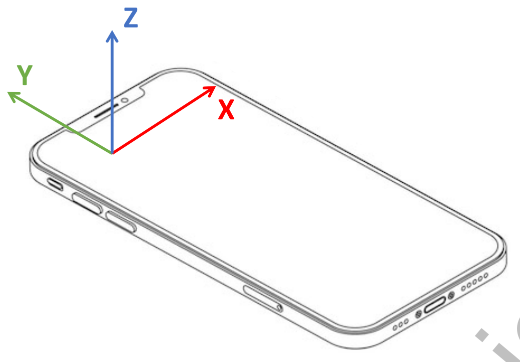

Fig. 3. Coordinate system for magnetic sensing on mobile

To understand the field distribution of Halbach magnets, we perform a simple case study. We place the Halbach magnet on the origin of the orientate system and move the phone around the 2D plane to measure the strength and direction of the field, as illustrated in Fig. 4(a). The result is shown in Fig. 4(b), where the direction of each arrow represents the direction of magnetic field at a given position and the length of the arrow is the log of the field strength.

In Fig. 4(b), we can observe that the strength decays nearly monotonically as the distance to the magnet increases. However, the direction of magnetic field has complex patterns and the field is asymmetric on different orientations of the magnet. This hints that when the magnet moves with the finger, the field may exhibit unique patterns for different gesture movement. Therefore, the wearable magnet may provide a means to recognize complex finger movements.

3.4 Multi-finger Gesture Design

Using the Halbach magnet, we are able to attach multiple magnets to different fingers and distinguish the movement of each individual finger. As shown in Fig. 4(b), different sides of the magnet produce magnetic fields of different directions. Therefore, we propose placing Halbach magnets with different orientations on different fingers to distinguish each finger. In the experiment, we place one magnet on the index finger of the left hand, its front side, as shown in Fig. 1(a), facing upwards, while the other magnet is placed on the middle finger with the back side, as shown in Fig. 1(b), facing upwards.

Constraints makes different magnet orientations exhibit different magnetic signal patterns when the same gesture is performed by different fingers. First, since the magnetometer on the mobile phone is installed at the up-left corner, it's impractical to attach the magnets to the right hand, which is too far from the magnetometer. Thus, we place the magnets on fingers of the left hand. Therefore, the fingers can only approach the sensor from the left, the top, the front, or the bottom. Considering the risk of tapping the screen or being mistaken as a different finger approaching from the bottom, we avoid gestures involving fingers approaching from the front. Second, the magnets are attached to the index finger and the middle finger, so the magnets wouldn't flip because of finger movements, whereas If we place a magnet on the thumb, its side facing upwards can change resulting from movements of the thumb.

To verify our gesture design, we attach Halbach magnets with different orientations on the index and middle finger and capture the signal pattern when fingers swipe up and down. As shown in Fig. 5, the magnetic field changes in the XY-plane when gestures are performed by different fingers. The X and Y-axis are the strength of magnetic fields of the given axis measured in terms μT. The traces are represented by a sequence of magnet field

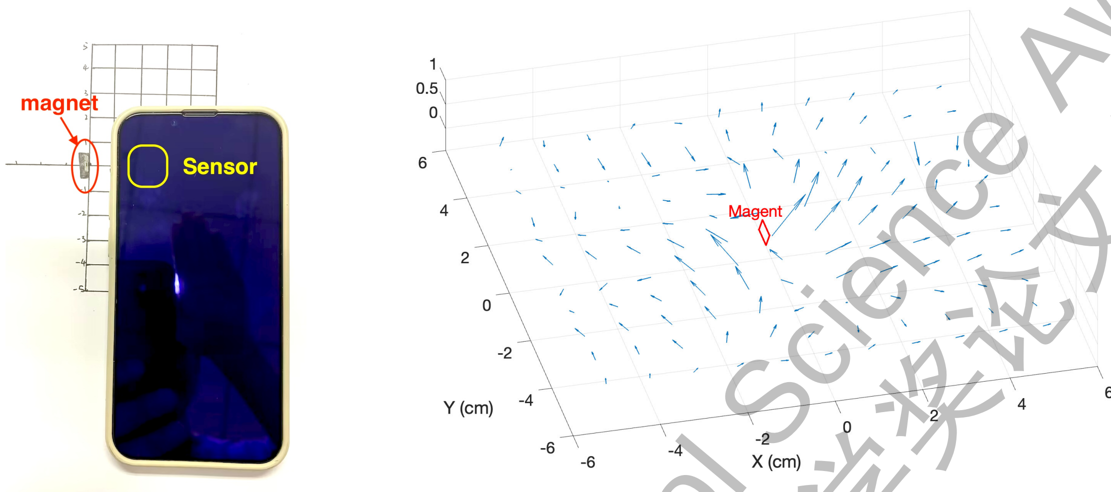

(a) Measurement Process

(b) 3D Magnetic field distribution

Fig. 4. Magnetic field distribution measurement of Halbach magnet

change vectors, each as the change for a 33.3 millisecond interval. We can see that all traces start and end at the origin, which means the magnetic field of the Halbach magnet is close to zero when fingers are far to the sensor. When performing the swiping, the finger first moves closer to the sensor and then moves away. Therefore, the amplitude of the magnetic field first increases and then decreases. A closer look at Fig. 5 would reveal the difference in gesture patterns that are related to the different movements. First, for the swiping down gesture (the blue and yellow trace), the traces of both the index finger and the middle finger are counter-clockwise. The corresponding swiping up gesture is the reverse activity of swiping down, so the red and purple traces are similar to the blue and yellow ones, except the fact that the arrows point in the opposite direction. Therefore, we can determine whether the user is swiping down or swiping up by seeing whether the trace is rotating counter-clockwise or clockwise. Second, the magnets on the index finger and the middle finger are placed in different orientations. Hence, the directions of the magnet's poles are different. Therefore, the index finger mostly induces a positive magnetic field along the Y-axis (H_y), while the middle finger induces a negative field along the Y-axis. Moreover, due to the asymmetric nature of the Halbach magnet, the field of magnet on middle finger is considerably larger than that of the magnet on the index finger at the measured position. The magnitude of field also varies depending on the distance between the finger and the sensor when performing the gesture.

By analyzing the traces above, we deduce the following conclusions on the magnetic field patterns. The field direction changes are the key to sensing different types of gestures and distinguishing between different fingers. The magnitude of the field isn't as important as the direction, since it is largely influenced by the distance between the magnet and the magnetometer. Therefore, we may need to normalize the strength of the magnetic field before performing recognition. The regular and smooth pattern of the magnetic trace also hints that it is possible to design fine-grained gestures. For example, the direction of the magnetic field is related to the angle of the finger. We can see that the angle between the finger and the side of the phone monotonically increase or decrease when performing the swiping up/down gesture. Therefore, by measuring the angle at a given time instance, we can determine the exact position of the finger along the swiping path.

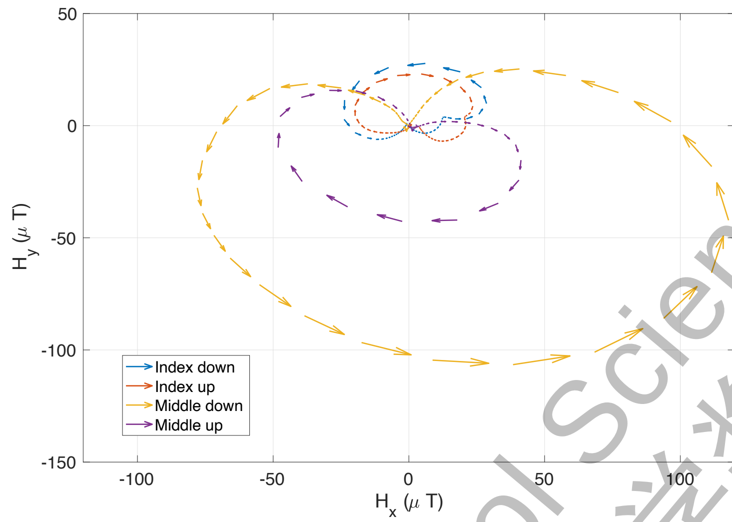

Fig. 5. Magnetic field pattern of different finger movements.

(a) Tapping top (T) (b) Tapping left (L) (c) Tapping bottom (B) (d) Swiping up (U) (e) Swiping down (D)

Fig. 6. Gesture Design

Based on the observations above, we design five gestures for each finger: tapping the top side of the phone (T), tapping the left side of the phone (L), tapping the bottom of the phone (B), swiping up (U), and swiping down (D), as shown in Fig. 6. These five gestures can be performed by either the index finger or the middle finger, so we have ten gestures in total. We use double letter codes to represent both the gesture and the finger performing the gesture. For example, "LI" means tapping the left side of the phone using the index finger and "DM" means swiping down using the middle finger. Each of these gestures generates a unique magnetic field change pattern that can be easily recognized. These gestures serve as our basic gesture set. However, our multi finger wearable approach opens many opportunities for new gesture design and we will discuss these opportunities in Sec. 6.

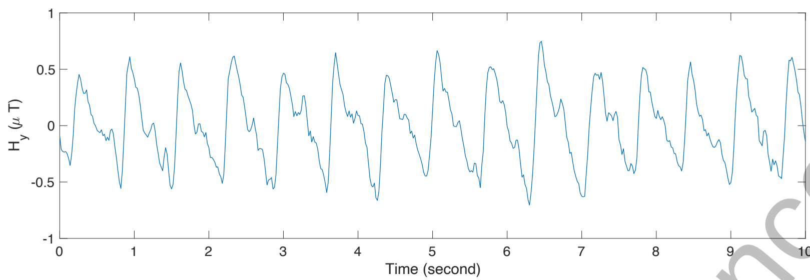

Fig. 7. Captured pulse signal on fingertip

3.5 Gesture Extensions

During our experiments on wearable magnets, we discover an interesting phenomenon. When the finger with a Halbach magnet rests statically on the surface of the device, we can clearly observe regular ups-and-downs in the magnetic field strength. Fig. 7 shows the magnetic measurement, which resembles the heartbeat signals captured by PhotoPlethysmoGraphy (PPG) sensors [31, 32]. We can clearly observe the regular peaks in the magnetic field strength, which has a peak-to-valley difference of around 1 μT. We can count about 15 peaks in the waveform that has a duration of 10 seconds, which converts to around 90 beats per minute (BPM).

The reason for the change in in the magnetic field could be that the pulse of the user leads to small vibrations on the finger tip, in a similar manner as the ballistocardiogram (BCG) [33]. Due to the fast magnetic field change of the Halbach magnet within a short distance, as shown in Fig. 2, a small movement of the finger tip caused by the heartbeat would lead to a large change change in the magnetic field. Therefore, it is possible to pickup the pulse signal by resting the finger tip attached with the Halbach magnet on the surface of the device. Note that the source of heartbeat signal is possibly different to the induced biomagnetic field that used in [34].

With the capability of the sensing the pulse signal, we envision that wearable magnets can be used for applications that are not limited to gesture recognition. First, many mobile devices, such as smart watch, VR/AR, and earphones, already are equipped with the magnetometer. Therefore, the wearable magnet approach can potentially supplant the high-cost PPG sensors in these devices to measure the heart rate and other health-related information. Second, the pulse signal captured by the wearable-magnet approach has a relative good quality so that they may be used for applications such as user authentication. As the heartbeat pattern for a given user has unique features [35], it is possible to identify the user through the magnetic pulse signal. Therefore, with the wearable magnet, the device can authenticate the user by asking the user to place the finger on the device before starting a session. In this project, we try to estimate the heartbeat rate signal from the above magnetic readings and leave the heartbeat-based authentication as the future work.

4 SYSTEM DESIGN

4.1 System Overview

The overall processing procedure of this project is shown in Fig. 8. Our system first collects both the IMU data (including the 3-axis accelerometer and the gyroscope readings) and the magnetometer data with a rate of 50 readings per second. Then, we perform data calibration to remove the background magnetic field using both the IMU and the magnetometer data. After that, we detect gesture movements based on the amplitude of the magnetic field in three axes. Signals containing gesture movements are then segmented for further processing. The first step for signal processing is noise removal. We use to moving average approach to remove fast fluctuations. If we detect that the user placed the finger tip statically on the devices, we will further use a detrending algorithm to

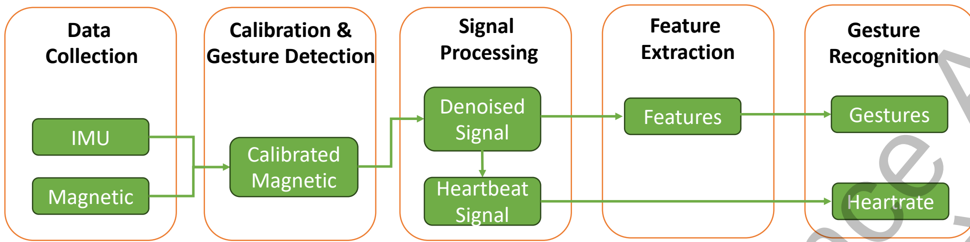

Fig. 8. System overview

extract the small changes caused by heartbeat for heart rate estimation. The gesture signal then goes through the feature extraction process to get the feature vectors for gesture recognition. Finally, we use a simple nearest neighbor matching algorithm to recognize the gesture performed.

4.2 Calibration and Gesture Detection

The readings of the magnetometer are susceptible to interference, including nearby iron objects and the Earth's magnetic field. Before capturing the magnetic field introduced by the finger movement, we need to first remove the magnetic field background. Most existing magnetometer calibration solutions either require the users to move the device in a given way or use complex hardware with multiple magnetometers [6]. In this project, we use a simple calibration approach. We observe that in most cases, the users do not move the device while performing the gesture. Therefore, we use the IMU readings to help the calibration. When the changes of the accelerometer and gyroscope are small, we treat the device as not moving. We record the magnetic field during a period when the device is not moving and use the average of the readings as the background magnetic field. If the device moves, we will treat the background magnetic field as unavailable and use the previous background as reference. In this case, the previous background could differ to the true background by the amount of the earth magnetic field, which is 22~65 μT.

We detect the gesture movement by comparing the amplitude of magnetic field to a threshold. We use different thresholds under different cases. When the device is not moving, we use a low threshold (*e.g.*, 10 μT) to detect if the user is performing a gesture. This gives a high detection rate as shown in Sec. 5. In the case of movement, as the magnetic field background is unavailable, the detection threshold is higher (*e.g.*, 60 μT). So, we can detect about 60% gestures with the higher threshold. Once the magnetic signal amplitude is higher than the threshold, a potential gesture is detected and we record the signals from previous 2 seconds (100 samples) and perform further signal processing. When the magnetic field is strong and the change in the field strength is small, the system will think that user may place the fingertip statically on the surface of the device. In this case, the system will start the process to extract the heartbeat signal from the magnetic readings.

4.3 Signal Processing

The raw magnetic measurements are noisy as shown in Fig. 9(a). While we can observe regular changes (pulse signals in this case), there are small irregular noises in the signal. These noises affect both the later gesture recognition and the heart rate estimation. So, we use a simple moving average filter to smooth the signal. For an input signal sequence of $x(n)$, the smoothed signal $y(n)$ is represented as:

$$y(n) = \frac{1}{k} \sum_{i=0}^{k-1} x(n+i). \tag{1}$$

Therefore, the output $y(n)$ is the average of the next k input samples. This smoothing is performed separately for each sequence in the readings for the X, Y, and Z axis. The length of the window, k, determines the smoothness of the output signal. A larger k makes the output smoother. In practice, we choose to use a k value of 10, which means average over a window of around 0.2 seconds. Fig. 9(b) shows the smoothed result, where the heartbeat peaks become more obvious.

The denoised signal can be directly used for gesture recognition. However, we can see that there are slow up-and-down trends in Fig. 9(b), which is caused by unintentional small movements of the user's fingers. Such slow trending interfere with the heart rate estimation task. Therefore, we perform an extra trend removal process for heart rate estimation. We first use a moving window average with a large value of k to estimate the trend. As human heartbeat is around once to twice per second, we choose to average over a window of one second ($k = 50$). In this way, the heartbeat changes will be smoothed out in such a long window and only the trend remains. We can then subtract the trend from the original signal and get the heartbeat signal. As shown in Fig. 9(c), the heartbeat signal without trend has very regular peaks and valleys. Therefore, we can use a simple peak detection algorithm to detect each heartbeat and get the heart rate estimation.

4.4 Feature Extraction

We extract different types of features from a segment of magnetic readings to be used as features for gesture recognition. Most gestures last around 1 second in our design. Therefore, we choose to derive the signal features from a signal segment with a fixed number of N samples, where we set N as 80 (around 1.6 seconds for 50 samples per second). As observed from Fig. 5, the magnitude of the signal is less important than the direction of the field. So, we first perform a normalization on the signal segment, by dividing every sample by the maximum magnetic amplitude in the segment. Therefore, the largest sample in the segment always has an amplitude of 1. We also subtract the average readings along each axis to let the average be zero, which is required when calculating the Pearson correlation coefficient mentioned later.

There are many different ways to construct the feature vector. The simplest way is just concatenate all the X, Y, Z readings into a big vector. In other word, for a segment of $N = 80$ samples, we will get a vector of $80 \times 3 = 240$ float point values. We also convert the original (H_x, H_y, H_z) readings into spherical coordinates (r, θ, ϕ), where:

$$r = \sqrt{H_x^2 + H_y^2 + H_z^2}, \tag{2}$$
$$\theta = \arccos(H_z/r), \tag{3}$$
$$\phi = \arctan(H_y/H_x). \tag{4}$$

However, we find that using the spherical coordinates do not perform as well as the using original (H_x, H_y, H_z) as shown in Sec. 5.

4.5 Gesture Recognition

Based on our gesture design, most of the gestures have distinctive signal patterns. Therefore, we can directly compare the captured signal with gesture patterns to find the gesture that the feature vector belongs to. We measure the similarity of two feature vectors A and B using the Pearson correlation coefficient, defined as:

$$\rho_{AB} = \frac{A \cdot B}{||A|| \times ||B||}, \tag{5}$$

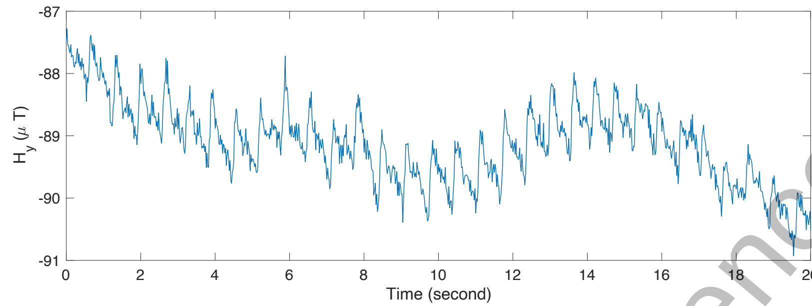

(a) Raw signal for 20 seconds of heartbeat

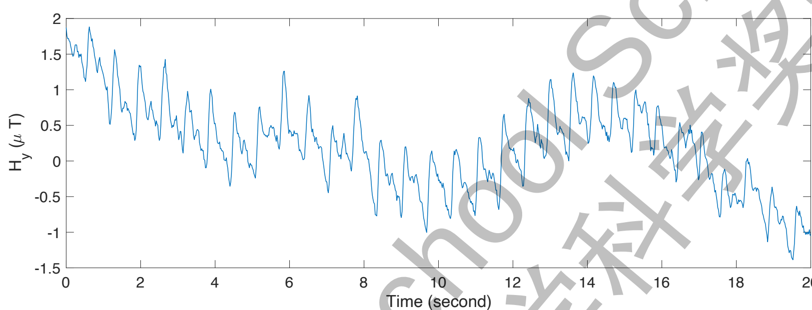

(b) Smoothed signal

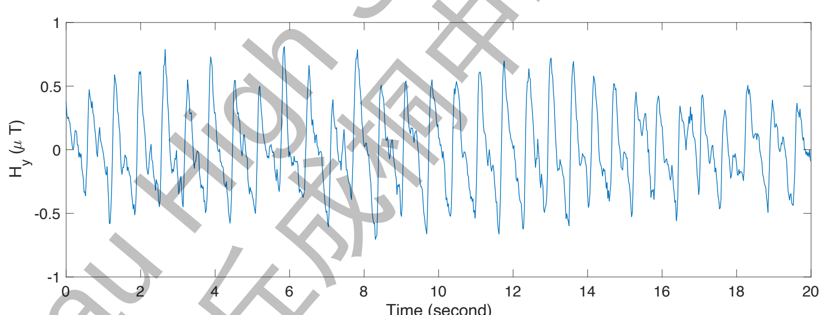

(c) After removing the trend

Fig. 9. Signal processing for magnetic readings

where $||\cdot||$ means the L2-norm of the given vector. The correlation coefficient is just the dot product of the two features normalized by their length. It provides a value between -1 and 1, which shows the similarity of the two vectors. Two identical feature vector will have a correlation coefficient of 1. And, two exactly opposite vector will have a value of -1. Therefore, we can record sample templates for each type of gestures, and compute the correlation coefficient of the captured signal to each template. If the capture signal is close to one of the templates, *i.e.*, having a ρ larger than a given threshold, then we can determine that the signal is similar to the given gesture.

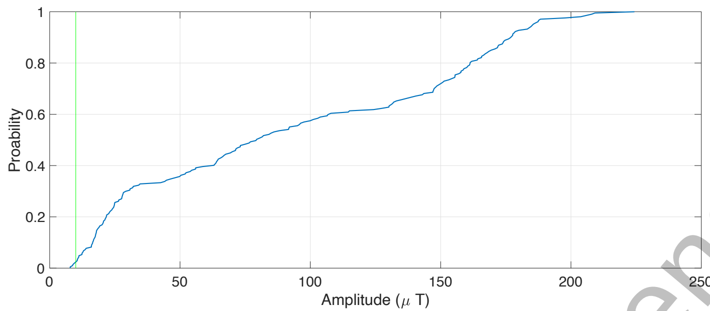

Fig. 10. Cumulative distribution function of the gesture amplitude

We usually select the gesture with the largest correlation coefficient as the output, which is similar as the nearest neighbor matching.

In practice, we find out that directly cutting one segment and matching it to the templates often leads to errors. Therefore, we use a sliding window in the match. After detected the gesture, we use a window of N samples to generate the feature vector and calculate the correlation coefficient to each gesture template. We keep moving the sliding window and find the maximum ρ for each template. We compare the maximum ρ to determine the final gesture recognition result. The sliding window approach provides better performance as indicated by our experimental results in Sec. 5.

5 IMPLEMENTATION AND EXPERIMENTS

5.1 Implementation and Data Collection

We implemented an offline data analysis system. We collect the IMU and magnetometer readings using the measurement applications available on iOS. The data is saved in plain text using the CVS format and transferred to a laptop for offline processing. We collected more than 200 gesture samples in total, with around 20 samples for each of the ten gestures. The offline processing program runs on MATLAB, which performs the data processing, gesture detection, data analysing, and draws the result. The offline processing program takes about 300~400 lines of code in MATLAB.

In the data collection process, two Halbach magnets with different orientations are attached to the index finger and the middle finger of the user. The user then performs different sets of gestures with different fingers in two sessions. In each session, one particular gesture is repeated by about ten times and the collected data are segmented and labeled offline.

5.2 Experimental Results

5.2.1 Gesture Detection. To evaluate the performance of our gesture detection scheme and determine the detection threshold, we plot the maximum amplitude changes of the magnetic field for all gesture samples. Fig. 10 shows the Cumulative Distribution Function (CDF) of the magnetic field. We observe that more than 60% of the gestures introduce magnetic field changes higher than 50 μT, which is larger than the peak of the Earth's magnetic field. However, to reliably detect all gestures, we set the detection threshold to 10 μT as shown by the green line in Fig. 10, which leads to a detection rate of 97.6%.

5.2.2 Gesture Recognition. Fig. 11 shows the correlation coefficient of ten different gestures, where a dark color means high correlation. We observe that for the gesture samples in the same group, the correlation coefficient

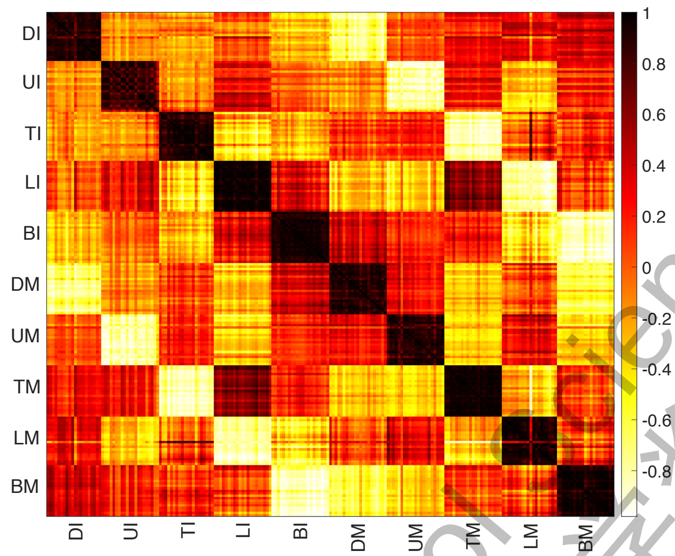

Fig. 11. Correlation coefficient of gesture signals using the sliding window approach

has high values that are close to 1. The correlations between different gestures are small. Especially, for the same gesture performed by different fingers, *e.g.*, swiping down by the middle finger and index finger (DM and DI), we can clearly observe negative correlations close to -1. This means with the opposite magnet orientation, the same gesture produce a nearly opposite magnetic field change for different fingers.

The distinctive correlation patterns leads to a high recognition accuracy for our simple nearest neighbor matching based on the correlation coefficient. We use one sample for each gesture type as the template and test the rest samples against the template. We use the label of the template with highest correlation coefficient as the output label. In our evaluation, we rotate the samples used for templates and repeat the test for 20 times so that each sample acts as the template once. The overall recognition accuracy for this approach is 99.14%. This shows the simple matching algorithm is sufficient for our task.

We also perform evaluation on other alternative solutions. Fig. 12(a) shows the performance of using the spherical coordinates (r, θ, ϕ) as the features. This approach provides good distinctions for swiping up and down, since, as indicated by our previous Fig. 5, they have exactly the opposite direction changes. However, for other gestures, the correlation pattern is not that clear. This approach leads to a worse accuracy of 78.53% as shown in Tab. 1. This is somehow surprising as normally we think the direction is a much better indication of the gesture movement.

Fig. 12(b) shows the performance when we do not use the sliding window to find the highest correlation point and just align samples by their highest peaks. We observe that without the sliding window, the swiping gestures has lower correlation inside the same type of gestures. The reason for this could be that the peaks of the signal, which depends on the closest point of the trajectory to the device, may not provide a good alignment for long-range movements such as swiping. The recognition accuracy without the sliding window matching is just 84.36%.

5.2.3 Heart Rate Estimation. To evaluate the performance of our heartbeat sensing scheme, I collect heartbeat signal by placing my index finger on the surface of the phone. The total length of the collected data is 289

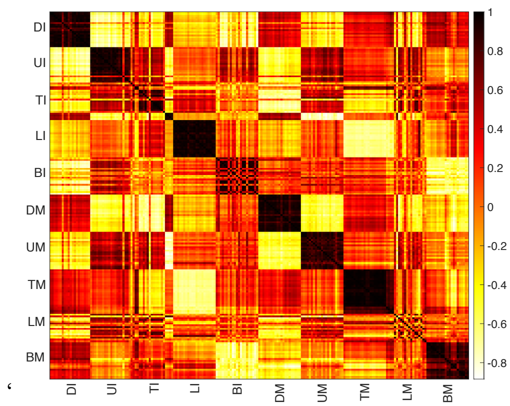

(a) Spherical coordinate features

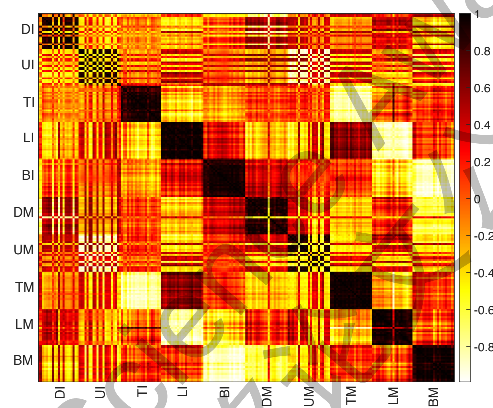

(b) Without sliding window matching

Fig. 12. Correlation coefficient of other methods

Table 1. Gesture recognition accuracy

Approach	Accuracy
Cartesian coordinate with sliding window	**99.14**
Spherical coordinate with sliding window	78.53
Cartesian coordinate without sliding window	84.36

seconds and our peak detection scheme find 389 heartbeats in the data set. Fig. 13(a) shows the interval between detected heartbeats. We observe most heartbeats have intervals between 0.6 and 0.8 seconds. The average of all measurements is 0.7281 seconds, which coverts to a heart rate estimation of 82.4 beats per minute (BPM). This is quite close to my own heart rate at 75~85 BPM. Among the 389 detected heartbeats, only 18 heartbeats have large errors in heartbeat intervals. Most error centers around 1.2~1.4 seconds, which are mainly caused by missing one heartbeat in between. By calculating the reciprocal of the interval for each heartbeat, we can get the heart rate estimation from a single heartbeat. Fig. 13(b) shows the estimation result, we observe that the per beat estimation is also quite accurate, with most estimations distributed around 80 BPM. The ones with large errors could be easily filted out, as they mostly are quite small (less than 50 BPM).

6 LIMITATION AND DISCUSSIONS

We have provided some preliminary results in using wearable magnets to perform gesture recognition and heartbeat sensing. However, due to the limited time, we have not explored the full potential of wearable magnetic sensing. We summarize the limitation of our work as follows.

Gesture Design: In this project, we only use two orientations to distinguish two fingers, while only one finger is performing the gesture in most cases. However, with the different design of Halbach structure, we can generate much more complex magnetic fields and place the magnet with other orientations. It would be interesting to find out if we can attach more magnets and allow multiple fingers to interact with each other. This would leads to more flexible gesture designs. Furthermore, from Fig. 5, we observe that the movement trace is regular and almost has a one-to-one correspondence of finger angle to the magnetic angle. Therefore, it could be possible to

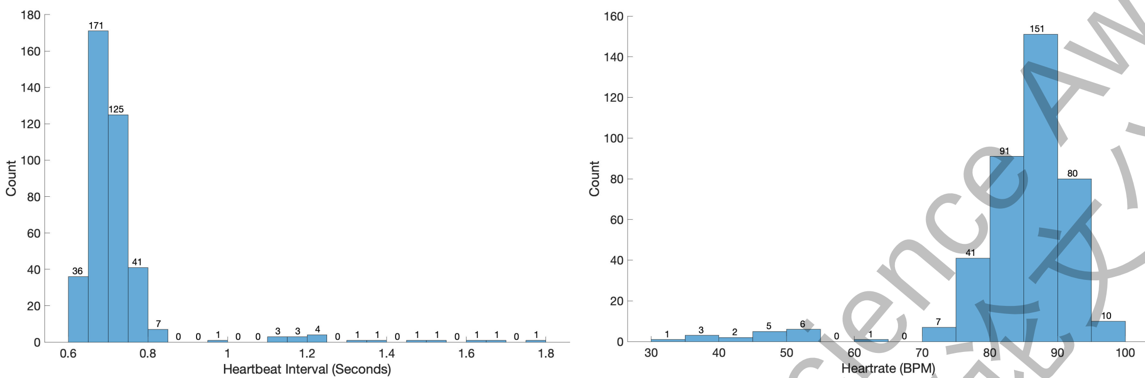

(a) Heartbeat interval distribution

(b) Estimated heart rate distribution

Fig. 13. Performance of heart rate estimation

measure the exact angle of finger movement and allow the objects on the screen to follow the movement of the finger. Such types of interaction would facilitate many tasks. We also intend to use the fingers as a fast text input method, but the design is not finalized.

Gesture Recognition Pipeline: We have used a simple correlation coefficient value to perform gesture recognition, which has limited extensibility and accuracy. A better design would use recent deep learning systems, *Transformers*, to perform the recognition task. However, due to the limited number of gesture samples collected, we are unable to train a sophisticated network in this project.

Multiple Magnetic Sensors: We only use a single magnetometer on the device. In the future, there could be multiple magnetometers on a single device. In this case, it would be easier to calibrate the magnetic field and we can use the difference between sensor to further improve the accuracy of gesture tracking.

Extension of the Heartbeat Sensing: In this project, we only demonstrated the possibility of sensing the heartbeat using wearable magnets. How to use this capability to perform user authentication or enabling new applications would be an interesting future work.

7 CONCLUSION

In this project, we have demonstrated the possibility of using wearable Halbach magnets to identify multi-finger gestures on mobile devices. We show that the ultra-thin Halbach magnets have unique magnetic properties that can help gesture recognition. With the wearable magnet, it is also possible to detect heartbeat signals through magnetic fields. We hope that the wearable magnet solution introduced in this project would open new possibilities for users to interact with mobile devices.

REFERENCES

[1] Dan Wu, Ruiyang Gao, Youwei Zeng, Jinyi Liu, Leye Wang, Tao Gu, and Daqing Zhang. FingerDraw: Sub-wavelength level finger motion tracking with WiFi signals. *Proceedings of the ACM on Interactive, Mobile, Wearable and Ubiquitous Technologies*, 4(1):1–27, 2020.

[2] Vladimir I Pavlovic, Rajeev Sharma, and Thomas S. Huang. Visual interpretation of hand gestures for human-computer interaction: A review. *IEEE Transactions on pattern analysis and machine intelligence*, 19(7):677–695, 1997.

[3] Sungjae Hwang, Andrea Bianchi, Myungwook Ahn, and Kwangyun Wohn. MagPen: magnetically driven pen interactions on and around conventional smartphones. In *Proceedings of the 15th international conference on Human-computer interaction with mobile devices and services*, pages 412–415, 2013.

[4] Chris Harrison and Scott E Hudson. Abracadabra: wireless, high-precision, and unpowered finger input for very small mobile devices. In *Proceedings of the 22nd annual ACM symposium on User interface software and technology*, pages 121–124, 2009.

[5] Kent Lyons. Wearable magnetic field sensing for finger tracking. In *Proceedings of the ACM International Symposium on Wearable Computers*, pages 63–67, 2020.

[6] Mingke Wang, Qing Luo, Yasha Iravantchi, Xiaomeng Chen, Alanson Sample, Kang G Shin, Xiaohua Tian, Xinbing Wang, and Dongyao Chen. Automatic calibration of magnetic tracking. In *Proceedings of the 28th Annual International Conference on Mobile Computing And Networking (MobiCom)*, pages 391–404, 2022.

[7] Andrea Bianchi and Ian Oakley. MagnID: Tracking multiple magnetic tokens. In *Proceedings of the 9th International Conference on Tangible, Embedded, and Embodied Interaction*, pages 61–68, 2015.

[8] Clement Zheng, Jeeeun Kim, Daniel Leithinger, Mark D Gross, and Ellen Yi-Luen Do. Mechamagnets: Designing and fabricating haptic and functional physical inputs with embedded magnets. In *Proceedings of the 13th International Conference on Tangible, Embedded, and Embodied Interaction*, pages 325–334, 2019.

[9] Jiha Kim, Younho Nam, Jungeun Lee, Young-Joo Suh, and Inseok Hwang. ProxiFit: Proximity magnetic sensing using a single commodity mobile toward holistic weight exercise monitoring. *Proceedings of the ACM on Interactive, Mobile, Wearable and Ubiquitous Technologies (IMWUT)*, 7(3):1–32, 2023.

[10] Sang Ho Yoon, Ke Huo, and Karthik Ramani. TMotion: Embedded 3D mobile input using magnetic sensing technique. In *Proceedings of the 10th International Conference on Tangible, Embedded, and Embodied Interaction*, pages 21–29, 2016.

[11] Yihao Liu, Kai Huang, Xingzhe Song, Boyuan Yang, and Wei Gao. Maghacker: eavesdropping on stylus pen writing via magnetic sensing from commodity mobile devices. In *Proceedings of the 18th international conference on mobile systems, applications, and services (MobiSys)*, pages 148–160, 2020.

[12] Kent Lyons. 2D input for virtual reality enclosures with magnetic field sensing. In *Proceedings of the ACM International Symposium on Wearable Computers*, pages 176–183, 2016.

[13] Lihao Wang, Wei Wang, Haipeng Dai, and Shizhe Liu. MagSound: Magnetic field assisted wireless earphone tracking. *Proceedings of the ACM on Interactive, Mobile, Wearable and Ubiquitous Technologies*, 7(1):1–32, 2023.

[14] AS Jouda, Ali Makki Sagheer, and Moceheb Lazam Shuwandy. MagRing-SASB: Static authentication of magnetism sensor using semi-biometric interaction magnetic ring. In *the 11th International Conference on System Engineering and Technology (ICSET)*, pages 183–188. IEEE, 2021.

[15] Yiting Zhang, Ming Yang, Zhen Ling, Yaowen Liu, and Wenjia Wu. FingerAuth: 3D magnetic finger motion pattern based implicit authentication for mobile devices. *Future Generation Computer Systems*, 108:1324–1337, 2020.

[16] Keunwoo Park, Daehwa Kim, Seongkook Heo, and Geehyuk Lee. Magtouch: Robust finger identification for a smartwatch using a magnet ring and a built-in magnetometer. In *Proceedings of the 2020 CHI Conference on Human Factors in Computing Systems*, pages 1–13, 2020.

[17] Mehran Roshandel, Aarti Munjal, Peyman Moghadam, Shahin Tajik, and Hamed Ketabdar. Multi-sensor based gestures recognition with a smart finger ring. In *the 16th International Conference on HCI*, pages 316–324. Springer, 2014.

[18] Liwei Chan, Rong-Hao Liang, Ming-Chang Tsai, Kai-Yin Cheng, Chao-Huai Su, Mike Y Chen, Wen-Huang Cheng, and Bing-Yu Chen. FingerPad: private and subtle interaction using fingertips. In *Proceedings of the 26th annual ACM symposium on User interface software and technology*, pages 255–260, 2013.

[19] Ke-Yu Chen, Kent Lyons, Sean White, and Shwetak Patel. uTrack: 3D input using two magnetic sensors. In *Proceedings of the 26th annual ACM symposium on User interface software and technology*, pages 237–244, 2013.

[20] Xing-Dong Yang, Tovi Grossman, Daniel Wigdor, and George Fitzmaurice. Magic finger: always-available input through finger instrumentation. In *Proceedings of the 25th annual ACM symposium on User interface software and technology*, pages 147–156, 2012.

[21] Gabriel Reyes, Jason Wu, Nikita Juneja, Maxim Goldshtein, W Keith Edwards, Gregory D Abowd, and Thad Starner. Synchrowatch: One-handed synchronous smartwatch gestures using correlation and magnetic sensing. *Proceedings of the ACM on Interactive, Mobile, Wearable and Ubiquitous Technologies*, 1(4):1–26, 2018.

[22] DoYoung Lee, Jiwan Kim, and Ian Oakley. Fingertext: Exploring and optimizing performance for wearable, mobile and one-handed typing. In *Proceedings of the 2021 CHI conference on human factors in computing systems*, pages 1–15, 2021.

[23] Ke-Yu Chen, Shwetak N Patel, and Sean Keller. Finexus: Tracking precise motions of multiple fingertips using magnetic sensing. In *Proceedings of the 2016 CHI Conference on Human Factors in Computing Systems*, pages 1504–1514, 2016.

[24] Rajalakshmi Nandakumar, Vikram Iyer, Desney Tan, and Shyamnath Gollakota. FingerIO: Using active sonar for fine-grained finger tracking. In *Proceedings of ACM CHI*, 2016.

[25] Teng Wei and Xinyu Zhang. mTrack: High-precision passive tracking using millimeter wave radios. In *Proceedings of ACM MobiCom*, 2015.

[26] Hong Li, Wei Yang, Jianxin Wang, Yang Xu, and Liusheng Huang. WiFinger: Talk to your smart devices with finger-grained gesture. In *Proceedings of ACM International Joint Conference on Pervasive and Ubiquitous Computing*, pages 250–261, 2016.

[27] Xing-Dong Yang, Khalad Hasan, et al. Around-device finger input on commodity smartwatches with learning guidance through discoverability. *International Journal of Human-Computer Studies*, 179:103105, 2023.

[28] Zimo Liao, Zhicheng Luo, Qianyi Huang, Linfeng Zhang, Fan Wu, Qian Zhang, and Yi Wang. SMART: screen-based gesture recognition on commodity mobile devices. In *Proceedings of the 27th Annual International Conference on Mobile Computing and Networking (MobiCom)*, pages 283–295, 2021.

[29] Katia Vega and Hugo Fuks. Beauty tech nails: interactive technology at your fingertips. In *Proceedings of the 8th international conference on tangible, embedded and embodied interaction*, pages 61–64, 2014.

[30] Bill Tao, Emerson Sie, Jay Shenoy, and Deepak Vasisht. Magnetic backscatter for in-body communication and localization. In *Proceedings of the 29th Annual International Conference on Mobile Computing and Networking (MobiCom)*, pages 1–15, 2023.

[31] Andrew Reisner, Phillip A Shaltis, Devin McCombie, H Harry Asada, David S Warner, and Mark A Warner. Utility of the photoplethysmogram in circulatory monitoring. *The Journal of the American Society of Anesthesiologists*, 108(5):950–958, 2008.

[32] Benoit Henry, Maxime Merz, Harry Hoang, Ghaith Abdulkarim, Jedrek Wosik, and Patrick Schoettker. Cuffless blood pressure in clinical practice: challenges, opportunities and current limits. *Blood Pressure*, 33(1):2304190, 2024.

[33] David Friedrich, Xavier L Aubert, Hartmut Führ, and Andreas Brauers. Heart rate estimation on a beat-to-beat basis via ballistocardiography-a hybrid approach. In *2010 Annual International Conference of the IEEE Engineering in Medicine and Biology*, pages 4048–4051. IEEE, 2010.

[34] Xiuzhen Guo, Long Tan, Tao Chen, Chaojie Gu, Yuanchao Shu, Shibo He, Yuan He, Jiming Chen, and Longfei Shangguan. Exploring biomagnetism for inclusive vital sign monitoring: Modeling and implementation. In *Proceedings of the 30th Annual International Conference on Mobile Computing and Networking*, pages 93–107, 2024.

[35] Lei Wang, Kang Huang, Ke Sun, Wei Wang, Chen Tian, Lei Xie, and Qing Gu. Unlock with your heart: Heartbeat-based authentication on commercial mobile phones. *Proceedings of the ACM on interactive, mobile, wearable and ubiquitous technologies*, 2(3):1–22, 2018.

ACKNOWLEDGMENT

I would like to thank everyone that help me in this project. Without their support and encouragement, it would be unimaginable for me to finish this project.

First and foremost, I would like to thank my project adviser, Dr. Shu Li, from Nanjing Foreign Language School. Dr. Shu Li has been teaching me computer science for four years during my study in NFLS. From Dr. Li's courses, I learned most of my computer knowledge, including programming, algorithm design and analysis skills. In this project, Dr. Li participated from the beginning, right after I got the initial idea of gesture recognition. He helped me in formulation of basic designs, solving technical challenges, and paper writing. I would also like to thank other NOI coaches and friends from NFLS for their helps in improving my programming skills.

Second, I would like to thank Professor Zhuzhong Qian from the School of Computer Science in Nanjing University, who is my supervisor for the National Scientific and Technological Innovation Talent Training Program (YinCaiJiHua) supported by CAST and MOE. While Prof. Qian does not directly participate in this project, he provides essential training on research skills that I applied in this project, including problem formulating, data collection/analysis, and paper writing/presentation. Through the YinCaiJiHua Project, Prof. Qian introduced me to the academic research area of computer science and provides many valuable research resources. I would also like to thank all the faculties, TAs and peer students participated in the YinCaiJiHua in NJU for their insightful discussions and suggestions to this project.

This project start roughly at May, 2024, when I thought of attaching devices to the fingers to perform gesture recognition. After surveyed recent papers, I found that this topic is popular in the HCI area and there are many existing solutions. However, most battery-less solutions use permanent magnets or magnetic devices that are too large for the finger. Fortunately, I found the Halbach magnets from Honor mobiles which are small and thin. Therefore, I may build a system with magnets attached to fingers that is different from existing solutions. In this way, I have a rough project plan for the summer vacation by the end of June. In July, I tried different ways to wear the magnets on fingers and different gestures. I found that it is quite easy to distinguish fingers with different magnets. I also found that the signal is sensitive enough to measure the heartbeat in July. In August, I finalized my gesture design and collected/processed the data around the middle of the August. Due to the limitation of my time, there are many things that I wished to do but cannot be finished before the deadline, which is listed in the discussion and limitations section.